Systems & Control Letters 63 (2014) 12–24

Contents lists available at ScienceDirect

Systems & Control Letters

journal homepage: www.elsevier.com/locate/sysconle

Distributed control of angle-constrained cyclic formations using bearing-only measurements

Shiyu Zhao [a], Feng Lin [b], Kemao Peng [b], Ben M. Chen [a,*], Tong H. Lee [a]

[a] Department of Electrical and Computer Engineering, National University of Singapore, Singapore

[b] Temasek Laboratories, National University of Singapore, Singapore

ARTICLE INFO

Article history:
Received 15 October 2012
Received in revised form
6 October 2013
Accepted 7 October 2013

Keywords:
Bearing-only measurement
Formation control
Cyclic formation
Finite-time stability
Lyapunov approach

ABSTRACT

This paper studies distributed control of multi-vehicle formations with angle constraints using bearing-only measurements. It is assumed that each vehicle can only measure the local bearings of their neighbors and there are no wireless communications among the vehicles. The desired formation is a cyclic one, whose underlying information flow is described by an undirected cycle graph. We propose a distributed bearing-only formation control law that ensures local exponential or finite-time stability. Collision avoidance between any vehicles can be locally guaranteed in the absence of inter-vehicle distance measurements.

1. Introduction

1.1. Motivation and related work

In this paper we investigate distributed control of multi-vehicle formations with angle constraints using bearing-only measurements. Our research is motivated by *vision-based formation control* of ground and aerial vehicles [1–4]. In vision-based formation control problems, there are usually no wireless communications among the vehicles; each vehicle can only observe their neighbors through a passive sensor, camera. As long as a vehicle can localize its neighbors in the image taken by the camera using pattern recognition algorithms (see, for example, [5, Section V]), the relative bearings of its neighbors can be easily calculated given the intrinsic parameters of the camera [6, Section 3.3]. As a comparison, it would be much harder to obtain inter-vehicle distances from images. Detailed vision techniques are out of the scope of this paper. To sum up, since bearings can be easily obtained from vision while distances are not, formation control using bearing-only measurements provides a novel and practical framework for vision-based formation control tasks.

Multi-vehicle formation control has been studied extensively under various settings up to now. We next review related studies from the following two aspects, which are crucial to characterize a formation control problem. The first aspect is: what kinds of measurements are used for formation control? In conventional formation control problems, it is commonly assumed that each vehicle can obtain the *positions* of their neighbors via, for example, wireless communications. It is notable that the position information inherently consists of two kinds of partial information: *bearing* and *distance*. Formation control using bearing-only [7–12] or distance-only measurements [13,14] has become an active research topic in recent years. The second aspect is: how the desired formation is constrained? In recent years, control of formations with inter-vehicle distance constraints has become a hot research topic [15–20]. Recently researchers also investigated control of formations with bearing/angle constraints [8–12,21]. Formations with a mix of bearing and distance constraints has also been studied by [22,23].

From the point of view of the above two aspects, the problem studied in this paper can be stated as *control of formations with angle constraints using bearing-only measurements*. This problem is a relatively new research topic. Up to now only a few special cases have been solved. The work in [7] proposed a distributed control law for balanced circular formations of unit-speed vehicles. The proposed control law can globally stabilize balanced circular formations using bearing-only measurements. The work in [8–10] studied distributed control of formations of three or four vehicles using bearing-only measurements. The

* Corresponding author. Tel.: +65 65162289; fax: +65 67791103.
E-mail addresses: shiyuzhao@nus.edu.sg (S. Zhao), linfeng@nus.edu.sg (F. Lin), kmpeng@nus.edu.sg (K. Peng), bmchen@nus.edu.sg (B.M. Chen), eleleeth@nus.edu.sg (T.H. Lee).

0167-6911/$ – see front matter © 2013 Elsevier B.V. All rights reserved.
http://dx.doi.org/10.1016/j.sysconle.2013.10.003

global stability of the proposed formation control laws was proved by employing the Poincare–Bendixson theorem. But the Poincare–Bendixson theorem is only applicable to the scenarios involving only three or four vehicles. The work in [11] investigated formation shape control using bearing measurements. Parallel rigidity was proposed to formulate bearing-based formation control problems. A bearing-based control law was designed for a formation of three nonholonomic vehicles. Based on the concept of parallel rigidity, the research in [12] proposed a distributed control law to stabilize bearing-constrained formations using bearing-only measurements. However, the proposed control law in [12] requires communications among the vehicles. That is different from the problem considered in this paper where we assume there are no communications between any vehicles and each vehicle cannot share their bearing measurements with their neighbors. The work in [21,23] designed control laws that can stabilize generic formations with bearing (and distance) constraints. However, the proposed control laws in [21,23] require position instead of bearing-only measurements. In summary, although several frameworks have been proposed in [22,11,12,23] to solve bearing-related formation control tasks, it is still an open problem to design a control law that can stabilize generic bearing-constrained formations using bearing-only measurements.

1.2. Challenges

A number of challenging theoretical problems have arisen in bearing-based formation control. An important one is how to properly utilize the bearing measurements for control. There are generally two approaches. The first approach is that each vehicle uses its bearing measurements to estimate/track the positions of their neighbors. One may refer to [24] for bearing-only target tracking algorithms. Once the neighbors' positions have been estimated, they can be used for control. Hence in the first approach, the formation control is still based on position information and conventional control laws can be applied. But several problems need to be noticed. Firstly, since the positions are estimated from bearings, this approach leads to a coupled nonlinear estimation and control problem, whose stability needs to be rigorously analyzed. Secondly, position tracking using bearing-only measurements requires certain observability conditions, details of which are out of the scope of this paper. Intuitively speaking, in order to localize a vehicle from bearing measurements, we need to measure the bearings of the vehicle from different angles. However, most of the practical formation control tasks require relative static vehicle positions. Without relative motion, it is theoretically impossible for a vehicle to estimate its neighbors' positions from bearings. As a result, considering this limitation of the first approach, we will follow [8,11] and adopt the second approach, which is to directly implement formation control laws based on bearing measurements.

Collision avoidance is a key issue in all kinds of formation control tasks. This issue is especially important in bearing-only formation control as inter-vehicle distances are unmeasurable and uncontrollable. In order to prove collision avoidance, we need to analyze the dynamics of the inter-vehicle distances in the absence of distance measurements. As will be shown later, the distance- and angle-dynamics of the formation are strongly coupled with each other. To rigorously prove the formation stability, we need to analyze the two dynamics simultaneously. Furthermore, asymptotic convergence of the angle-dynamics would be insufficient to analyze the distance-dynamics. It is necessary to prove exponential or finite-time convergence rate, which makes the problem more challenging.

Another challenging and interesting problem is the scale control of a formation. In fact, the scale of a formation is uncontrollable with bearing-only measurements, and inter-vehicle distance measurements are required to control the formation scale. One possible approach to formation scale control is to consider mixed bearing and distance constraints/measurements. We will leave formation scale control for future research. In this paper we will not consider distance measurements or constraints. Finally, global stability analysis of bearing-based formation control undoubtedly is a challenging and meaningful research topic. When position measurements are available for formation control, a globally stable control law has been proposed in [25] to stabilize formations in arbitrary dimensions with fixed topology. However, when only bearing measurements are available, up to now control laws that guarantee global stability are only applicable to formations of three or four vehicles [8–10].

1.3. Contributions

As a first step towards solving generic bearing-based formation control, the work in this paper studies an important special case, cyclic formation, whose underlying information flow is described by an undirected cycle graph. In a cyclic formation, each vehicle has exactly two neighbors. The angle subtended at each vehicle by their two neighbors is pre-specified in the desired formation. The control objective is to steer each vehicle in the plane such that the angles converge to the pre-specified values. The main contributions of this paper are summarized as below.

(i) We propose a distributed control law that can stabilize cyclic formations merely using local bearing measurements. Compared to the existing work [8,10], the proposed control law can handle cyclic formations with an *arbitrary* number of vehicles. In addition, this paper does not make parallel rigidity assumptions [22,21,11] on the desired formation.
(ii) We prove in a unified way that the proposed control law ensures local exponential or finite-time stability. The exponential or finite-time stability can be easily switched by tuning a parameter in the control law. The stability analysis is based on Lyapunov approaches and significantly different from those in [8,10].
(iii) The dynamics of the inter-vehicle distances is analyzed in the absence of distance measurements. It is proved that the distance between any vehicles can neither approach zero nor infinity. Collision avoidance between any vehicles (no matter if they are neighbors or not) can be locally guaranteed.

If the vehicle number is larger than three, the shape of a cyclic formation would be indeterminate. To well define the shape of a formation of more than three vehicles, more complicated underlying graphs of the formation, such as rigid graphs, are required. More complicated cases are out of the scope of this paper and will be studied in the future.

1.4. Organization

The paper is organized as follows. Notations and preliminaries are presented in Section 2. The control objective and proposed control law are given in Section 3. The main results of this paper, the basic and advanced analyses of the formation stability, are presented in Sections 4 and 5, respectively. Simulations are given in Section 6 to verify the effectiveness and robustness of the control law. Conclusions are drawn in Section 7.

2. Notations and preliminaries

2.1. Notations

The eigenvalues of a symmetric positive semi-definite matrix $A \in \mathbb{R}^{n\times n}$ are denoted as $0 \le \lambda_1(A) \le \lambda_2(A) \le \cdots \le \lambda_n(A)$. Let $\mathbf{1} = [1, \ldots, 1]^{\mathrm{T}} \in \mathbb{R}^n$, and I be the identity matrix with

appropriate dimensions. Denote $[\cdot]_{ij}$ as the entry at the ith row and jth column of a matrix, and $[\cdot]_i$ as the ith entry of a vector. Let $|\cdot|$ be the absolute value of a real number, and $\|\cdot\|_p$ be the p-norm of a vector. For the sake of simplicity, we omit the subscript when $p = 2$, i.e., denoting $\|\cdot\|$ as the 2-norm. The null space of a matrix is denoted as Null $(\cdot)$. The angle between two vectors is denoted as $\angle(\cdot,\cdot)$.

Given an arbitrary angle $\alpha \in \mathbb{R}$, the 2 by 2 rotation matrix

$$R(\alpha) = \begin{bmatrix} \cos\alpha & -\sin\alpha \\ \sin\alpha & \cos\alpha \end{bmatrix}$$

geometrically rotates a vector in $\mathbb{R}^2$ counterclockwise through an angle α about the origin. It is easy to see that for all nonzero $x \in \mathbb{R}^2$: (i) $x^{\mathrm{T}}R(\alpha)x > 0$ when $\alpha \in (-\pi/2, \pi/2) \pmod{2\pi}$; (ii) $x^{\mathrm{T}}R(\alpha)x = 0$ when $\alpha = \pm\pi/2 \pmod{2\pi}$; (iii) and $x^{\mathrm{T}}R(\alpha)x < 0$ when $\alpha \in (\pi/2, 3\pi/2) \pmod{2\pi}$. Moreover, we have $R^{-1}(\alpha) = R^{\mathrm{T}}(\alpha) = R(-\alpha)$ and $R(\alpha_1)R(\alpha_2) = R(\alpha_1 + \alpha_2)$ for arbitrary angles α_1 and α_2. Finally, for any $x \in \mathbb{R}^2$, denote $x^{\perp} = R(\pi/2)x$. Clearly $x^{\mathrm{T}}x^{\perp} = 0$.

2.2. Graph theory

An *undirected graph* $\mathcal{G} = (\mathcal{V}, \mathcal{E})$ consists of a vertex set $\mathcal{V} = \{1, \ldots, n\}$ and an edge set $\mathcal{E} \subseteq \mathcal{V} \times \mathcal{V}$, where an edge is an unordered pair of distinct vertices. The undirected edge between vertices i and j is denoted as (i, j) or (j, i). If $(i, j) \in \mathcal{E}$, then i and j are called to be adjacent. A path from i to j in a graph is a sequence of distinct nodes starting with i and ending with j such that consecutive vertices are adjacent. If there is a path between any two vertices in $\mathcal{G}$, then $\mathcal{G}$ is said to be connected. The set of neighbors of vertex i is denoted as $\mathcal{N}_i = \{j \in \mathcal{V} : (i, j) \in \mathcal{E}\}$. An undirected *cycle* is a connected graph where every vertex has exactly two neighbors.

An *orientation* of an undirected graph is the assignment of a direction to each edge. An *oriented graph* is an undirected graph together with a particular orientation. A directed edge (i, j) in the oriented graph points from vertex i to vertex j. The *incidence matrix* E of an oriented graph is the $\{0, \pm1\}$-matrix with rows indexed by edges and columns by vertices. More specifically, suppose (j, k) is the ith directed edge of the oriented graph. Then the entry of E in the ith row and kth column is 1, the one in the ith row and jth column is -1, and the others in the ith row are zero. Thus we have $E\mathbf{1} = 0$ by definition. Moreover, if the graph is connected, we have rank$(E) = n-1$ [26, Theorem 8.3.1] and hence Null $(E) =$ span$\{\mathbf{1}\}$.

2.3. Useful lemmas

We next prove and introduce some useful results.

Lemma 1. *Let $\mathcal{U} \triangleq \{x \in \mathbb{R}^n : x \neq 0$ and nonzero entries of x are not of the same sign $\}$. Suppose $A \in \mathbb{R}^{n\times n}$ is a positive semi-definite matrix with $\lambda_1(A) = 0$ and $\lambda_2(A) > 0$. If $\mathbf{1} = [1, \ldots, 1]^{\mathrm{T}} \in \mathbb{R}^n$ is an eigenvector associated with the zero eigenvalue of A, then*

$$\inf_{x\in\mathcal{U}} \frac{x^{\mathrm{T}}Ax}{x^{\mathrm{T}}x} = \frac{\lambda_2(A)}{n}.$$

Proof. See Appendix A.

Remark 1. By the definition of $\mathcal{U}$, any $x \in \mathcal{U}$ should at least contain one positive entry and one negative entry. If the nonzero entries of x are all positive or negative, then $x \notin \mathcal{U}$.

Lemma 2. *Let $x(t)$ be a real positive scalar variable of $t \in [0, +\infty)$. Given any positive constants α and k, if the time derivative of $x(t)$ satisfies*

$$|\dot{x}(t)| \leq \alpha \exp\left(\int_0^t -\frac{k}{x(\tau)}\mathrm{d}\tau\right), \quad t \in [0, +\infty), \tag{1}$$

then $x(t)$ for all $t \in [0, +\infty)$ has a finite upper bound.

Proof. See Appendix B.

Lemma 3 (*[27, Lemma 2]*). *Let $x_1, \ldots, x_n \geq 0$. Given $p \in (0, 1]$, then*

$$\left(\sum_{i=1}^n x_i\right)^p \leq \sum_{i=1}^n x_i^p \leq n^{1-p}\left(\sum_{i=1}^n x_i\right)^p.$$

Lemma 4 (*[28, Corollary 5.4.5]*). *Let $\|\cdot\|_\alpha$ and $\|\cdot\|_\beta$ be any two vector norms on $\mathbb{R}^n$. Then there exist finite positive constants C_m and C_M such that $C_m\|x\|_\alpha \leq \|x\|_\beta \leq C_M\|x\|_\alpha$ for all $x \in \mathbb{R}^n$.*

3. Problem formulation

3.1. Control objective

Consider n ($n \geq 3$) vehicles in $\mathbb{R}^2$. Denote the position of vehicle i as $z_i \in \mathbb{R}^2$. The dynamics of each vehicle is modeled as

$$\dot{z}_i = u_i,$$

where $u_i \in \mathbb{R}^2$ is the control input to be designed. This paper focuses on cyclic formations (see Fig. 1), whose underlying information flow is described by an undirected cycle graph. In a cyclic formation, each vehicle has exactly two neighbors. Denote θ_i as the angle at vehicle i subtended by its two neighbors (see Fig. 1). The angle θ_i is specified as $\theta_i^* \in [0, 2\pi)$ in the desired formation. The desired angles $\{\theta_i^*\}_{i=1}^n$ should be feasible such that there exist $\{z_i\}_{i=1}^n$ ($z_i \neq z_j$ for $i \neq j$) to realize the desired formation. We make the following assumptions on $\{\theta_i^*\}_{i=1}^n$ and $\{z_i(0)\}_{i=1}^n$.

Assumption 1. In the desired formation, $\theta_i^* \neq 0$ and $\theta_i^* \neq \pi$ for all $i \in \{1, \ldots, n\}$.

Remark 2. Assumption 1 means no three consecutive vehicles in the desired formation are collinear. The collinear case is a theoretical difficulty in many formation control problems (see, for example, [16,17,20,10]). In practice, bearings are usually measured by optical sensors such as cameras. Hence vehicle i cannot measure the bearings of its two neighbors simultaneously when $\theta_i = 0$ due to line-of-sight occlusion. On the other hand, the field-of-view of a monocular camera is usually less than 180 degrees. Hence vehicle i cannot measure the bearings of its two neighbors simultaneously either when $\theta_i = \pi$ due to limited field-of-view. Thus Assumption 1 is reasonable from the practical point of view.

Assumption 2. In the initial formation, no two vehicles coincide with each other, i.e., $z_i(0) \neq z_j(0)$ for all $i \neq j$.

The formation control objective is summarized as below.

Problem 1. Under Assumptions 1 and 2, design control input u_i for vehicle i ($i = 1, \ldots, n$) based only on the local bearing measurements of its two neighbors such that the formation is steered from its initial position $\{z_i(0)\}_{i=1}^n$ to a finite final position $\{z_i(t_f)\}_{i=1}^n$ where $\theta_i(t_f) = \theta_i^*$. The final converged time t_f can be either infinite or finite. During the formation evolution, collision avoidance between any vehicles should be guaranteed.

3.2. Control law design

We next define some notations and then propose our formation control law. In the cyclic formation, we can have $\mathcal{N}_i = \{i-1, i+1\}$ for $i \in \{1, \ldots, n\}$ by indexing the vehicles properly (see Fig. 1).

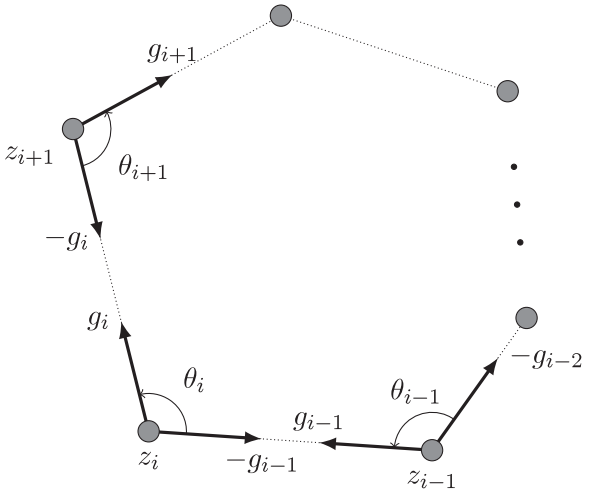

Fig. 1. An illustration of cyclic formations.

Then vehicle i can measure the bearings of vehicles $i-1$ and $i+1$. The indices $i+1$ and $i-1$ are taken modulo n. Denote

$$e_i \triangleq z_{i+1} - z_i \tag{2}$$

as the edge vector pointing from vehicle i to vehicle $i+1$. Then the unit-length vector

$$g_i \triangleq \frac{e_i}{\|e_i\|}$$

characterizes the relative bearing between vehicles $i+1$ and i (see Fig. 1). Thus the bearings measured by vehicle i include g_i and $-g_{i-1}$. The control input u_i will be designed as a function of g_i and $-g_{i-1}$.

The angle $\theta_i \in [0, 2\pi)$ is defined in the following way (see Fig. 1): rotating $-g_{i-1}$ counterclockwise through an angle θ_i about vehicle i yields g_i, which can be expressed as

$$g_i = R(\theta_i)(-g_{i-1}).$$

When θ_i is defined in the above way, the angles θ_i and θ_{i+1} are on the same side of e_i for all $i \in \{1, \ldots, n\}$. As a result, the quantity $\sum_{i=1}^n \theta_i$ is invariant to the positions of the vehicles because the sum of the interior or exterior angles of a polygon is constant. Thus if $\sum_{i=1}^n \theta_i(0) = \sum_{i=1}^n \theta_i^*$, then $\sum_{i=1}^n \theta_i(t) \equiv \sum_{i=1}^n \theta_i^*$.

The angle error for vehicle i, which will be used for feedback control, is defined as

$$\varepsilon_i \triangleq \cos\theta_i - \cos\theta_i^* = -g_i^{\mathrm{T}} g_{i-1} - \cos\theta_i^*. \tag{3}$$

The nonlinear control law for vehicle i is designed as

$$u_i = \mathrm{sgn}(\varepsilon_i)|\varepsilon_i|^a (g_i - g_{i-1}), \tag{4}$$

where $a \in (0, 1]$ and $\mathrm{sgn}(\varepsilon_i)$ is defined by

$$\mathrm{sgn}(\varepsilon_i) = \begin{cases} 1 & \text{if } \varepsilon_i > 0 \\ 0 & \text{if } \varepsilon_i = 0 \\ -1 & \text{if } \varepsilon_i < 0. \end{cases}$$

In the special case of $a = 1$, control law (4) becomes $u_i = \varepsilon_i(g_i - g_{i-1})$ because $\mathrm{sgn}(\varepsilon_i)|\varepsilon_i| = \varepsilon_i$.

Remark 3. It should be noted that $\mathrm{sgn}(\varepsilon_i)|\varepsilon_i|^a$ is *continuous* in ε_i for $a \in (0, 1]$. That is because $\lim_{\varepsilon_i \to 0^+} \mathrm{sgn}(\varepsilon_i)|\varepsilon_i|^a = \lim_{\varepsilon_i \to 0^-} \mathrm{sgn}(\varepsilon_i)|\varepsilon_i|^a = 0$. Therefore, the control law is continuous in ε_i and there are no chattering issues when ε_i varies around zero.

Remark 4. Note $a \neq 0$ in the control law. When $a = 0$, control law (4) will be discontinuous in ε_i. Then the stability analysis will rely on tools for discontinuous dynamic systems [29,30]. The discontinuous case of $a = 0$ is out of the scope of this paper.

Clearly (4) is a *distributed* control law as it only relies on the bearings of vehicle i's neighbors. Moreover, although g_i and g_{i-1} in (4) are expressed in a global coordinate frame, the control law can be implemented based on the local bearings measured in the local coordinate frame of vehicle i. To see that, denote R_i as the rotation transformation from a global frame to the local frame of vehicle i. Then the bearings of vehicles $i-1$ and $i+1$ measured in the local frame are $R_i(-g_{i-1})$ and $R_i g_i$, respectively. Note ε_i defined in (3) is invariant to R_i. Then substituting $R_i(-g_{i-1})$ and $R_i g_i$ into (4) gives $u_{i,\mathrm{local}} = \mathrm{sgn}(\varepsilon_i)|\varepsilon_i|^a R_i(g_i - g_{i-1})$. Converting $u_{i,\mathrm{local}}$ into the global frame would yield the same control input value given by (4).

As will be shown later, control law (4) ensures local exponential stability if $a = 1$, and local finite-time stability if $a \in (0, 1)$. Loosely speaking, finite-time stability means ε_i for all i converges to zero in finite time. See [31] or [32, Section 4.6] for a formal definition of finite-time stability of nonlinear systems. Besides fast convergence, finite-time stability can also bring benefits such as disturbance rejection and robustness against uncertainties [31,33,34]. In this paper, we will present a unified proof of the exponential and finite-time stability based on Lyapunov approaches.

4. Basic stability analysis

In this section, we first propose a continuously differentiable Lyapunov function and then show its time derivative under control law (4) is non-positive.

4.1. Lyapunov function

Denote $\varepsilon = [\varepsilon_1, \ldots, \varepsilon_n]^{\mathrm{T}} \in \mathbb{R}^n$ and $z = [z_1^{\mathrm{T}}, \ldots, z_n^{\mathrm{T}}]^{\mathrm{T}} \in \mathbb{R}^{2n}$. It is straightforward to see from (4) that $\varepsilon = 0$ implies $\dot{z} = 0$ and then $\dot{\varepsilon} = 0$. Hence $\varepsilon = 0$ is an equilibrium of the ε-dynamics. Consider the Lyapunov function

$$V(\varepsilon) = \frac{1}{a+1} \sum_{i=1}^n |\varepsilon_i|^{a+1}.$$

Clearly V is positive definite with respect to $\varepsilon = 0$. In the special case of $a = 1$, we have $V = 1/2\varepsilon^{\mathrm{T}}\varepsilon$, which is a quadratic function of ε.

We next show V is *continuously differentiable* in ε. (i) If $\varepsilon_i > 0$, $\frac{\partial|\varepsilon_i|^{a+1}}{\partial\varepsilon_i} = \frac{\partial\varepsilon_i^{a+1}}{\partial\varepsilon_i} = (a+1)\varepsilon_i^a = (a+1)\mathrm{sgn}(\varepsilon_i)|\varepsilon_i|^a$ and hence $\lim_{\varepsilon_i \to 0^+} \frac{\partial|\varepsilon_i|^{a+1}}{\partial\varepsilon_i} = 0$. (ii) If $\varepsilon_i < 0$, $\frac{\partial|\varepsilon_i|^{a+1}}{\partial\varepsilon_i} = \frac{\partial(-\varepsilon_i)^{a+1}}{\partial\varepsilon_i} = -(a+1)(-\varepsilon_i)^a = (a+1)\mathrm{sgn}(\varepsilon_i)|\varepsilon_i|^a$ and hence $\lim_{\varepsilon_i \to 0^-} \frac{\partial|\varepsilon_i|^{a+1}}{\partial\varepsilon_i} = 0$. From (i) and (ii) we have

$$\frac{\partial|\varepsilon_i|^{a+1}}{\partial\varepsilon_i} = (a+1)\mathrm{sgn}(\varepsilon_i)|\varepsilon_i|^a, \quad \forall \varepsilon_i \in \mathbb{R}. \tag{5}$$

Note $\mathrm{sgn}(\varepsilon_i)|\varepsilon_i|^a$ is continuous in ε_i for $a \in (0, 1]$. Thus $|\varepsilon_i|^{a+1}$ is continuously differentiable in ε_i. As a result, V is continuously differentiable in ε.

4.2. Time derivative of V

We next derive the time derivative of V under control law (4) and show it is non-positive. For the sake of simplicity, denote

$$\sigma_i \triangleq \mathrm{sgn}(\varepsilon_i)|\varepsilon_i|^a$$

and $\sigma = [\sigma_1, \ldots, \sigma_n]^{\mathrm{T}} \in \mathbb{R}^n$. Then control law (4) can be rewritten as $\dot{z}_i = \sigma_i(g_i - g_{i-1})$, and (5) becomes $\partial|\varepsilon_i|^{a+1}/\partial\varepsilon_i = (a+1)\sigma_i$. The time derivative of V is

$$\begin{aligned}
\dot{V} &= \frac{1}{a+1}\sum_{i=1}^{n}\frac{\partial|\varepsilon_i|^{a+1}}{\partial\varepsilon_i}\dot{\varepsilon}_i \\
&= \sum_{i=1}^{n}\sigma_i\dot{\varepsilon}_i \quad (\text{By (5)}) \\
&= \sum_{i=1}^{n}\sigma_i(-g_i^{\mathrm{T}}\dot{g}_{i-1} - g_{i-1}^{\mathrm{T}}\dot{g}_i) \quad (\text{By (3)}) \\
&= \sum_{i=1}^{n}\sigma_i(-g_i^{\mathrm{T}}\dot{g}_{i-1}) + \sum_{i=1}^{n}\sigma_i(-g_{i-1}^{\mathrm{T}}\dot{g}_i) \\
&= \sum_{i=1}^{n}\sigma_{i+1}(-g_{i+1}^{\mathrm{T}}\dot{g}_i) + \sum_{i=1}^{n}\sigma_i(-g_{i-1}^{\mathrm{T}}\dot{g}_i) \\
&= -\sum_{i=1}^{n}(\sigma_{i+1}g_{i+1} + \sigma_i g_{i-1})^{\mathrm{T}}\dot{g}_i. \qquad (6)
\end{aligned}$$

Since $g_i = e_i/\|e_i\|$, we have

$$\begin{aligned}
\dot{g}_i &= \frac{\dot{e}_i}{\|e_i\|} - \frac{e_i}{\|e_i\|^2}\frac{\mathrm{d}\|e_i\|}{\mathrm{d}t} \\
&= \frac{1}{\|e_i\|}\left(I - \frac{e_i}{\|e_i\|}\frac{e_i^{\mathrm{T}}}{\|e_i\|}\right)\dot{e}_i \triangleq \frac{1}{\|e_i\|}P_i\dot{e}_i, \qquad (7)
\end{aligned}$$

where $P_i = I - g_i g_i^{\mathrm{T}}$. Note P_i is an *orthogonal projection matrix* satisfying $P_i^{\mathrm{T}} = P_i$ and $P_i^2 = P_i$. It is straightforward to see that $\mathrm{Null}(P_i) = \mathrm{span}\{g_i\}$ and P_i is positive semi-definite because $x^{\mathrm{T}}P_i x = x^{\mathrm{T}}P_i^{\mathrm{T}}P_i x = \|P_i x\|^2 \geq 0$ for all $x \in \mathbb{R}^2$. Furthermore, from (2) and control law (4), we have

$$\begin{aligned}
\dot{e}_i &= \dot{z}_{i+1} - \dot{z}_i \\
&= \sigma_{i+1}g_{i+1} + \sigma_i g_{i-1} - (\sigma_{i+1} + \sigma_i)g_i. \qquad (8)
\end{aligned}$$

Because $P_i g_i = 0$, substituting the above $\dot{e}_i$ back into (7) gives

$$\dot{g}_i = \frac{1}{\|e_i\|}P_i(\sigma_{i+1}g_{i+1} + \sigma_i g_{i-1}).$$

Substituting the above $\dot{g}_i$ back into (6) yields

$$\begin{aligned}
\dot{V} &= -\sum_{i=1}^{n}\frac{1}{\|e_i\|}(\sigma_{i+1}g_{i+1} + \sigma_i g_{i-1})^{\mathrm{T}}P_i(\sigma_{i+1}g_{i+1} + \sigma_i g_{i-1}) \\
&\leq 0. \qquad (9)
\end{aligned}$$

Now we can claim the equilibrium $\varepsilon = 0$ is at least Lyapunov stable.

We next derive the matrix form of (9), which will be useful to prove exponential and finite-time stability. To do that, we need the following lemma.

Lemma 5. *Let $g_i^{\perp} = R(\pi/2)g_i$. It is obvious that $\|g_i^{\perp}\| = 1$ and $(g_i^{\perp})^{\mathrm{T}}g_i = 0$. Furthermore,*

(i) $P_i = g_i^{\perp}(g_i^{\perp})^{\mathrm{T}}$.

(ii) $(g_i^{\perp})^{\mathrm{T}}g_j = -(g_j^{\perp})^{\mathrm{T}}g_i$ *for all* $i \neq j$.

(iii) $(g_i^{\perp})^{\mathrm{T}}g_{i-1} = \sin\theta_i$. *As a result,* $(g_i^{\perp})^{\mathrm{T}}g_{i-1} > 0$ *if* $\theta_i \in (0, \pi)$; *and* $(g_i^{\perp})^{\mathrm{T}}g_{i-1} < 0$ *if* $\theta_i \in (\pi, 2\pi)$.

Proof. See Appendix C.

Substituting $P_i = g_i^{\perp}(g_i^{\perp})^{\mathrm{T}}$ as shown in Lemma 5(i) into (9) yields

$$\begin{aligned}
\dot{V} &= -\sum_{i=1}^{n}\frac{1}{\|e_i\|}\left((g_i^{\perp})^{\mathrm{T}}(\sigma_{i+1}g_{i+1} + \sigma_i g_{i-1})\right)^2 \\
&\leq -\frac{1}{\sum_{i=1}^{n}\|e_i\|}\sum_{i=1}^{n}\left(\sigma_{i+1}(g_i^{\perp})^{\mathrm{T}}g_{i+1} + \sigma_i(g_i^{\perp})^{\mathrm{T}}g_{i-1}\right)^2 \\
&= -\frac{1}{\sum_{i=1}^{n}\|e_i\|}\|\xi\|^2, \qquad (10)
\end{aligned}$$

where

$$\begin{aligned}
\xi &= \begin{bmatrix} \sigma_2(g_1^{\perp})^{\mathrm{T}}g_2 + \sigma_1(g_1^{\perp})^{\mathrm{T}}g_n \\ \vdots \\ \sigma_1(g_n^{\perp})^{\mathrm{T}}g_1 + \sigma_n(g_n^{\perp})^{\mathrm{T}}g_{n-1} \end{bmatrix} \\
&= \begin{bmatrix} (g_1^{\perp})^{\mathrm{T}}g_n & (g_1^{\perp})^{\mathrm{T}}g_2 & 0 & \cdots & 0 \\ 0 & (g_2^{\perp})^{\mathrm{T}}g_1 & (g_2^{\perp})^{\mathrm{T}}g_3 & \cdots & 0 \\ 0 & 0 & (g_3^{\perp})^{\mathrm{T}}g_2 & \cdots & 0 \\ \vdots & \vdots & \vdots & \ddots & \vdots \\ (g_n^{\perp})^{\mathrm{T}}g_1 & 0 & \cdots & 0 & (g_n^{\perp})^{\mathrm{T}}g_{n-1} \end{bmatrix} \\
&\quad \times \begin{bmatrix} \sigma_1 \\ \sigma_2 \\ \sigma_3 \\ \vdots \\ \sigma_n \end{bmatrix} \\
&= \underbrace{\begin{bmatrix} 1 & -1 & 0 & \cdots & 0 \\ 0 & 1 & -1 & \cdots & 0 \\ 0 & 0 & 1 & \cdots & 0 \\ \vdots & \vdots & \vdots & \ddots & \vdots \\ -1 & 0 & \cdots & 0 & 1 \end{bmatrix}}_{E \in \mathbb{R}^{n\times n}} \\
&\quad \times \underbrace{\begin{bmatrix} (g_1^{\perp})^{\mathrm{T}}g_n & 0 & 0 & \cdots & 0 \\ 0 & (g_2^{\perp})^{\mathrm{T}}g_1 & 0 & \cdots & 0 \\ 0 & 0 & (g_3^{\perp})^{\mathrm{T}}g_2 & \cdots & 0 \\ \vdots & \vdots & \vdots & \ddots & \vdots \\ 0 & 0 & \cdots & 0 & (g_n^{\perp})^{\mathrm{T}}g_{n-1} \end{bmatrix}}_{D \in \mathbb{R}^{n\times n}} \\
&\quad \times \begin{bmatrix} \sigma_1 \\ \sigma_2 \\ \sigma_3 \\ \vdots \\ \sigma_n \end{bmatrix}. \qquad (11)
\end{aligned}$$

The last equality above uses the fact that $(g_i^{\perp})^{\mathrm{T}}g_{i-1} = -(g_{i-1}^{\perp})^{\mathrm{T}}g_i$ given by Lemma 5(ii). Substituting (11) into (10) yields

$$\dot{V} \leq -\frac{1}{\sum_{i=1}^{n}\|e_i\|}\sigma^{\mathrm{T}}D^{\mathrm{T}}E^{\mathrm{T}}ED\sigma. \qquad (12)$$

Inequality (12) is very important and will be used to prove the exponential and finite-time stability of the control law in the next section. We would like to mention that D is a diagonal matrix and $E\mathbf{1} = 0$. It can be easily checked that E is the incidence matrix of an

oriented cycle graph. Thus we have $\text{rank}(E) = n-1$ [26, Theorem 8.3.1] and hence $\text{Null}(E^{\mathrm{T}}E) = \text{Null}(E) = \text{span}\{\mathbf{1}\}$.

5. Exponential and finite-time stability analysis

Based on inequality (12) obtained in the previous section, we next prove the exponential and finite-time stability of control law (4). The proof of our main result consists of three relatively independent steps, each of which will be summarized as a proposition. As aforementioned, the inter-vehicle distance dynamics is a theoretical difficulty. We will particularly analyze this issue in the second and third steps. More specifically, the second step shows that the distance between any two vehicles cannot approach infinity; the third step proves that the distance between any two vehicles (no matter if they neighbors or not) cannot approach zero during formation evolution.

At this point, it is still unclear whether any vehicles may collide with each other during formation evolution. Nevertheless, we can always assume there is a "collision time" $T_c \in (0, +\infty)$, at which at least two vehicles collide with each other. Note T_c could be infinity. If T_c is infinity, there would be no collision between any vehicles during the whole formation evolution. In fact, we will later prove T_c to be infinity given sufficiently small initial error ε_0. But at this point we are only able to claim that inequality (12) is valid only for $t \in [0, T_c)$.

Denote $\Omega(c) \triangleq \{\varepsilon \in \mathbb{R}^n : V(\varepsilon) \le c\}$ with $c > 0$ as the level set of $V(\varepsilon)$. Note V can be written as $V = 1/(a+1)\|\varepsilon\|_{a+1}^{a+1}$ where $\|\cdot\|_{a+1}$ is the $(a+1)$-norm. Hence $\Omega(c)$ is compact [28, Corollary 5.4.8]. Because $\dot V \le 0$ as shown in (12), the level set $\Omega(V(\varepsilon_0))$ is also positively invariant with respect to (4).

Proposition 1. *Under Assumptions 1 and 2, if the initial error ε_0 is sufficiently small, then there exists a positive constant K such that*

$$\dot V \le -\frac{K}{\sum_{i=1}^n \|e_i\|} V^{\frac{2a}{a+1}}, \quad \forall t \in [0, T_c). \tag{13}$$

Proof. Suppose $\varepsilon \ne 0 \Leftrightarrow \sigma \ne 0$. Rewrite $\sigma^{\mathrm{T}}D^{\mathrm{T}}E^{\mathrm{T}}ED\sigma$ on the right hand side of (12) as

$$\sigma^{\mathrm{T}}D^{\mathrm{T}}E^{\mathrm{T}}ED\sigma = \underbrace{\left(\frac{\sigma^{\mathrm{T}}D^{\mathrm{T}}E^{\mathrm{T}}ED\sigma}{\sigma^{\mathrm{T}}D^{\mathrm{T}}D\sigma}\right)}_{\text{term 1}} \underbrace{\left(\frac{\sigma^{\mathrm{T}}D^{\mathrm{T}}D\sigma}{V^{\frac{2a}{a+1}}}\right)}_{\text{term 2}} V^{\frac{2a}{a+1}}. \tag{14}$$

Step 1: analyze term 2 in (14). At the equilibrium point $\varepsilon = 0$ (i.e., $\theta_i = \theta_i^*$ for all i), we have $[D]_{ii} = (g_i^{\perp})^{\mathrm{T}}g_{i-1} \ne 0$ because $\theta_i^* \ne 0$ or π as stated in Assumption 1. Thus by continuity we have $[D]_{ii} \ne 0$ for every point in $\Omega(V(\varepsilon_0))$ if ε_0 is sufficiently small. Then $D^{\mathrm{T}}D = D^2$ is positive definite and hence $\lambda_1(D^{\mathrm{T}}D) > 0$ for all $\varepsilon \in \Omega(V(\varepsilon_0))$. Since $\Omega(V(\varepsilon_0))$ is compact, there exists a lower bound $\underline{\lambda}_1(D^{\mathrm{T}}D) > 0$ such that $\lambda_1(D^{\mathrm{T}}D) \ge \underline{\lambda}_1(D^{\mathrm{T}}D)$ and consequently

$$\sigma^{\mathrm{T}}D^{\mathrm{T}}D\sigma \ge \underline{\lambda}_1(D^{\mathrm{T}}D)\sigma^{\mathrm{T}}\sigma \tag{15}$$

for all $\varepsilon \in \Omega(V(\varepsilon_0))$. In addition, since $2a/(a+1) \in (0, 1]$, we have

$$\begin{aligned} V^{\frac{2a}{a+1}} &= \left(\frac{1}{a+1}\right)^{\frac{2a}{a+1}} \left(\sum_{i=1}^n |\varepsilon_i|^{a+1}\right)^{\frac{2a}{a+1}} \\ &\le \left(\frac{1}{a+1}\right)^{\frac{2a}{a+1}} \sum_{i=1}^n |\varepsilon_i|^{2a} \quad \text{(By Lemma 3)} \\ &= \left(\frac{1}{a+1}\right)^{\frac{2a}{a+1}} \sum_{i=1}^n \sigma_i^2 \quad (\text{By } |\varepsilon_i|^{2a} = \sigma_i^2) \\ &= \left(\frac{1}{a+1}\right)^{\frac{2a}{a+1}} \sigma^{\mathrm{T}}\sigma. \end{aligned} \tag{16}$$

Thus (15) and (16) imply

$$\begin{aligned} \frac{\sigma^{\mathrm{T}}D^{\mathrm{T}}D\sigma}{V^{\frac{2a}{a+1}}} &\ge \frac{\underline{\lambda}_1(D^{\mathrm{T}}D)\sigma^{\mathrm{T}}\sigma}{\left(\frac{1}{a+1}\right)^{\frac{2a}{a+1}}\sigma^{\mathrm{T}}\sigma} \\ &= (a+1)^{\frac{2a}{a+1}}\underline{\lambda}_1(D^{\mathrm{T}}D) \end{aligned} \tag{17}$$

for all $\varepsilon \in \Omega(V(\varepsilon_0)) \setminus \{0\}$.

Step 2: analyze term 1 in (14). Define

$$w_i = \frac{\cos\theta_i - \cos\theta_i^*}{\theta_i - \theta_i^*}.$$

Note $\lim_{\theta_i \to \theta_i^*} w_i = -\sin\theta_i^*$ by L'Hôpital's rule. Thus w_i is well defined even if $\theta_i - \theta_i^* = 0$. Denote $\delta_i \triangleq \theta_i - \theta_i^*$ and recall $\varepsilon_i = \cos\theta_i - \cos\theta_i^*$. Then we have $\varepsilon_i = w_i\delta_i$, whose matrix form is

$$\varepsilon = W\delta,$$

where $W = \text{diag}\{w_1, \ldots, w_n\} \in \mathbb{R}^{n\times n}$ and $\delta = [\delta_1, \ldots, \delta_n]^{\mathrm{T}} \in \mathbb{R}^n$. On one hand, when ε_0 is sufficiently small, we have θ_i is sufficiently close to θ_i^* such that both θ_i and θ_i^* are in either $(0, \pi)$ or $(\pi, 2\pi)$ for all $\varepsilon \in \Omega(V(\varepsilon_0))$. It can be examined that $w_i < 0$ when $\theta_i, \theta_i^* \in (0, \pi)$, and $w_i > 0$ when $\theta_i, \theta_i^* \in (\pi, 2\pi)$. On the other hand, $[D]_{ii} = (g_i^{\perp})^{\mathrm{T}}g_{i-1} > 0$ when $\theta_i \in (0, \pi)$, and $[D]_{ii} = (g_i^{\perp})^{\mathrm{T}}g_{i-1} < 0$ when $\theta_i \in (\pi, 2\pi)$ as shown in Lemma 5(iii). Thus we always have

$$[D]_{ii}w_i < 0$$

for all $i \in \{1, \ldots, n\}$ and all $\varepsilon \in \Omega(V(\varepsilon_0))$, which means the diagonal entries of DW *are of the same sign*. However, because $\sum_i^n \theta_i \equiv \sum_i^n \theta_i^* \Leftrightarrow \sum_{i=1}^n \delta_i = 0$, the nonzero entries in δ *are not of the same sign*. Hence the nonzero entries of $D\varepsilon = DW\delta$ *are not of the same sign*. Furthermore, because σ_i has the same sign as ε_i, the nonzero entries of $D\sigma$ *are not of the same sign* either. Thus $D\sigma \in \mathcal{U}$ where $\mathcal{U}$ is defined in Lemma 1. The above arguments are illustrated intuitively in Fig. 2. Recall $\text{Null}(E^{\mathrm{T}}E) = \text{Null}(E) = \text{span}\{\mathbf{1}\}$. Therefore, by Lemma 1 we have

$$\frac{\sigma^{\mathrm{T}}D^{\mathrm{T}}E^{\mathrm{T}}ED\sigma}{\sigma^{\mathrm{T}}D^{\mathrm{T}}D\sigma} > \frac{\lambda_2(E^{\mathrm{T}}E)}{n}. \tag{18}$$

Step 3: substituting (17) and (18) into (14) yields

$$\sigma^{\mathrm{T}}D^{\mathrm{T}}E^{\mathrm{T}}ED\sigma \ge \underbrace{\frac{\lambda_2(E^{\mathrm{T}}E)}{n}(a+1)^{\frac{2a}{a+1}}\underline{\lambda}_1(D^{\mathrm{T}}D)}_{K} V^{\frac{2a}{a+1}}. \tag{19}$$

Then (13) can be obtained by substituting (19) into (12). Note (12) holds for all $t \in [0, T_c)$, and so does (13). □

Proposition 1 requires ε_0 to be sufficiently small, but does not give any explicit condition of ε_0. In order to determine the region of convergence, we next give a *sufficient condition* of ε_0 which ensures the validity of Proposition 1. The proof of Proposition 1 requires ε_0 to be sufficiently small such that (i) $[D]_{ii} \ne 0$ and (ii) both θ_i and θ_i^* are in either $(0, \pi)$ or $(\pi, 2\pi)$ for all $\varepsilon \in \Omega(V(\varepsilon_0))$. Since $[D]_{ii} = 0$ if and only if $\theta_i = 0$ or π, condition (ii) implies condition (i). Denote $\Delta_i = \min\{\theta_i^*, |\theta_i^* - \pi|, 2\pi - \theta_i^*\}$ and $\bar\varepsilon_i = \min\{|\cos(\theta_i^* + \Delta_i) - \cos\theta_i^*|, |\cos(\theta_i^* - \Delta_i) - \cos\theta_i^*|\}$. Then we have the following sufficient condition. *If ε_0 satisfies*

$$V(\varepsilon_0) < \frac{1}{a+1}\min_i \bar\varepsilon_i^{a+1}, \tag{20}$$

$$\left.\begin{array}{l} DW\text{: same sign} \\ \delta\text{: not same sign} \end{array}\right\} \Longrightarrow DW\delta = D\varepsilon\text{: not same sign} \Longrightarrow D\sigma\text{: not same sign} \Longrightarrow D\sigma \in \mathcal{U}$$

Fig. 2. Illustrate how to obtain $D\sigma \in \mathcal{U}$.

then condition (ii) *can be satisfied and hence* Proposition 1 *is valid.* To see that, for any $j \in \{1, \ldots, n\}$, we have $\frac{1}{a+1}|\varepsilon_j(t)|^{a+1} \leq \frac{1}{a+1}\sum_{i=1}^{n}|\varepsilon_i(t)|^{a+1} = V(\varepsilon(t)) \leq V(\varepsilon_0) < \frac{1}{a+1}\min_i \bar{\varepsilon}_i^{a+1} \leq \frac{1}{a+1}\bar{\varepsilon}_j^{a+1}$. Thus $|\varepsilon_j(t)| < \bar{\varepsilon}_j$ for all $t \in [0, T_c)$. Since the cosine function is monotone in $(0, \pi)$ or $(\pi, 2\pi)$, we have $|\varepsilon_j(t)| < \bar{\varepsilon}_j \Longrightarrow |\theta_i(t) - \theta_i^*| < \Delta_i$ and hence condition (ii) is valid. It should be noted that $\Delta_i \neq 0$ because $\theta_i^* \neq 0$ or π. Therefore, $\bar{\varepsilon}_i > 0$ and hence the set of ε_0 that satisfies (20) is always nonempty.

Since the inter-vehicle distances are not controlled directly, we cannot simply rule out the possibility that $\sum_{i=1}^{n}\|e_i\|$ in (13) may go to infinity. Based on Proposition 1, we next further prove $\sum_{i=1}^{n}\|e_i\|$ is bounded above by a finite positive constant.

Proposition 2 (*Finite Inter-vehicle Distance*)**.** *Under Assumptions* 1 *and* 2*, if* (13) *holds and the initial error* ε_0 *is sufficiently small such that* $V(\varepsilon_0) \leq 1$*, then there exists a finite constant* $\gamma > 0$ *such that*

$$\sum_{i=1}^{n}\|e_i(t)\| \leq \gamma, \quad \forall t \in [0, T_c),$$

which holds even if $T_c = +\infty$*. As a result,* (13) *implies*

$$\dot{V} \leq -\frac{K}{\gamma}V^{\frac{2a}{1+a}}, \quad \forall t \in [0, T_c). \tag{21}$$

Proof. Denote $\rho(t) \triangleq \sum_{i=1}^{n}\|e_i(t)\|$ for the sake of simplicity. The time derivative of ρ is

$$\begin{aligned}
\dot{\rho} &= \sum_{i=1}^{n}\frac{\mathrm{d}\|e_i\|}{\mathrm{d}t} \\
&= \sum_{i=1}^{n} g_i^{\mathrm{T}}\dot{e}_i \\
&= \sum_{i=1}^{n} g_i^{\mathrm{T}}[\sigma_{i+1}(g_{i+1} - g_i) + \sigma_i(g_{i-1} - g_i)] \quad \text{(By (8))} \\
&= \sum_{i=1}^{n}[\sigma_{i+1}(g_i^{\mathrm{T}}g_{i+1} - 1) + \sigma_i(g_i^{\mathrm{T}}g_{i-1} - 1)] \\
&= \sum_{i=1}^{n}\sigma_i(g_{i-1}^{\mathrm{T}}g_i - 1) + \sum_{i=1}^{n}\sigma_i(g_i^{\mathrm{T}}g_{i-1} - 1) \\
&= 2\sum_{i=1}^{n}\sigma_i(g_i^{\mathrm{T}}g_{i-1} - 1) \\
&= v^{\mathrm{T}}\sigma,
\end{aligned}$$

where $v = [v_1, \ldots, v_n]^{\mathrm{T}} \in \mathbb{R}^n$ with $v_i = 2(g_i^{\mathrm{T}}g_{i-1} - 1)$. By the Cauchy–Schwarz inequality, we have

$$|\dot{\rho}| = |v^{\mathrm{T}}\sigma| \leq \|v\|\,\|\sigma\| \leq \beta\|\sigma\|, \tag{22}$$

where β is the maximum of $\|v\|$ over the compact set $\Omega(V(\varepsilon_0))$.

Furthermore, note

$$\begin{aligned}
V^{\frac{2a}{1+a}} &= \left(\frac{1}{a+1}\right)^{\frac{2a}{a+1}}\left(\sum_{i=1}^{n}|\varepsilon_i|^{a+1}\right)^{\frac{2a}{a+1}} \\
&\geq \left(\frac{1}{a+1}\right)^{\frac{2a}{a+1}}\frac{1}{n^{\frac{1-a}{1+a}}}\sum_{i=1}^{n}|\varepsilon_i|^{2a} \quad \text{(By Lemma 3)} \\
&= \left(\frac{1}{a+1}\right)^{\frac{2a}{a+1}}\frac{1}{n^{\frac{1-a}{1+a}}}\|\sigma\|^2,
\end{aligned}$$

which implies

$$\|\sigma\|^2 \leq \underbrace{(a+1)^{\frac{2a}{a+1}}n^{\frac{1-a}{1+a}}}_{\kappa}V^{\frac{2a}{a+1}}. \tag{23}$$

Substituting (23) into (22) yields

$$|\dot{\rho}| \leq \beta\sqrt{\kappa}V^{\frac{a}{a+1}}. \tag{24}$$

On the other hand, if ε_0 is sufficiently small such that $V(\varepsilon_0) \leq 1$, then $V^{\frac{2a}{1+a}} \geq V$ for all $\varepsilon \in \Omega(V(\varepsilon_0))$ as $2a/(1+a) \leq 1$. Thus (13) implies

$$\dot{V} \leq -\frac{K}{\rho}V^{\frac{2a}{1+a}} \leq -\frac{K}{\rho}V$$

for $\varepsilon \in \Omega(V(\varepsilon_0))$. By the comparison lemma [35, Lemma 3.4], the above inequality suggests

$$V(t) \leq V(0)\exp\left(\int_0^t -\frac{K}{\rho(\tau)}\mathrm{d}\tau\right). \tag{25}$$

Substituting (25) into (24) yields

$$|\dot{\rho}| \leq \beta\sqrt{\kappa}V(0)^{\frac{a}{a+1}}\exp\left(\int_0^t -\frac{\frac{a}{a+1}K}{\rho(\tau)}\mathrm{d}\tau\right). \tag{26}$$

Note (26) holds for $t \in [0, T_c)$.

Based on (26) we draw the following conclusions. (i) If T_c is infinity, (26) holds for $t \in [0, +\infty)$. By Lemma 2 there exists a finite constant that bounds $\rho(t)$ above for all $t \in [0, +\infty)$. (ii) If T_c is finite, it is obvious that $\rho(t)$ is finite for all $t \in [0, T_c)$ because the speed of each vehicle is finite. In either case, denote γ as the finite upper bound of ρ. Then it is evident to have (21) from (13). □

Remark 5. Since the formation is a cycle, the distance between any two vehicles (even they are not neighbors) is smaller than $\sum_{i=1}^{n}\|e_i\|$. Hence Proposition 2 implies that the distance between any vehicles is always finite during the whole formation evolution.

Collision avoidance is an important problem in various formation control tasks. It is especially important for bearing-based formation control as the inter-vehicle distances are unmeasurable and uncontrollable. Based on the results of Proposition 2, we next further prove no vehicles will collide with each other under control law (4) during the whole formation evolution.

Proposition 3 (*Collision Avoidance*)**.** *Under Assumptions* 1 *and* 2*, if* (21) *holds and the initial error* ε_0 *is sufficiently small such that* $V(\varepsilon_0) \leq 1$*, then there exists a positive constant* η *such that*

$$\sum_{i=1}^{n}\|z_i(t) - z_i(0)\| \leq \eta\|\varepsilon_0\|_{a+1}^{a}, \quad \forall t \in [0, T_c). \tag{27}$$

Furthermore, if ε_0 *satisfies*

$$\|z_j(0) - z_k(0)\| > \eta\|\varepsilon_0\|_{a+1}^{a} \tag{28}$$

for all $j, k \in \{1, \ldots, n\}$ and $j \neq k$, then $T_c = +\infty$ and the distance between any two vehicles is bounded below by a positive constant during the whole formation evolution.

Proof. We first prove (27). The quantity $\sum_{i=1}^{n} \|z_i(t) - z_i(0)\|$ actually characterizes the "distance" from the formation at time t to the initial formation. Recall

$$z_i(t) - z_i(0) = \int_0^t \sigma_i(g_i - g_{i-1})\mathrm{d}\tau$$

by control law (4). Then we have

$$\begin{aligned}
\sum_{i=1}^{n} \|z_i(t) - z_i(0)\| &= \sum_{i=1}^{n} \left\| \int_0^t \sigma_i(g_i - g_{i-1})\mathrm{d}\tau \right\| \\
&\leq \sum_{i=1}^{n} \int_0^t |\varepsilon_i|^a \|g_i - g_{i-1}\|\mathrm{d}\tau \\
&\leq 2\int_0^t \sum_{i=1}^{n} |\varepsilon_i|^a \mathrm{d}\tau \quad (\text{Because } \|g_i - g_{i-1}\| \\
&\quad \leq \|g_i\| + \|g_{i-1}\| = 2) \\
&\leq 2n^{1-a} \int_0^t \|\varepsilon(t)\|_1^a \mathrm{d}\tau \\
&\quad (\text{By Lemma 3}) \\
&\leq 2n^{1-a} C \int_0^t \|\varepsilon(t)\|_{a+1}^a \mathrm{d}\tau. \\
&\quad (\text{By Lemma 4}). \qquad (29)
\end{aligned}$$

If ε_0 is sufficiently small such that $V(\varepsilon_0) \leq 1$ and hence $V(t) \leq 1$ for all $t \in [0, T_c)$, then $V^{\frac{2a}{1+a}} \geq V$ as $2a/(1+a) \leq 1$. Consequently (21) implies

$$\dot{V} \leq -\frac{K}{\gamma} V^{\frac{2a}{1+a}} \leq -\frac{K}{\gamma} V,$$

which suggests

$$V(t) \leq V(0) e^{-\frac{K}{\gamma}t}, \quad \forall t \in [0, T_c). \qquad (30)$$

Substituting $V = 1/(a+1)\|\varepsilon\|_{a+1}^{a+1}$ into (30) yields

$$\|\varepsilon(t)\|_{a+1} \leq \|\varepsilon(0)\|_{a+1} e^{-\frac{K}{(a+1)\gamma}t}.$$

Substituting the above inequality into (29) gives

$$\begin{aligned}
\sum_{i=1}^{n} \|z_i(t) - z_i(0)\| &\leq 2n^{1-a} C \int_0^t \|\varepsilon(0)\|_{a+1}^a e^{-\frac{aK}{(a+1)\gamma}\tau} \mathrm{d}\tau \\
&= 2n^{1-a} C \|\varepsilon(0)\|_{a+1}^a \frac{(a+1)\gamma}{aK} \left(1 - e^{-\frac{aK}{(a+1)\gamma}t}\right) \\
&\leq \underbrace{\frac{2n^{1-a} C (a+1)\gamma}{aK}}_{\eta} \|\varepsilon(0)\|_{a+1}^a \qquad (31)
\end{aligned}$$

for all $t \in [0, T_c)$.

With the above preparation, we now prove collision avoidance by contradiction. Assume vehicles j and k collide at a *finite* time T_c, which means

$$z_j(T_c) = z_k(T_c). \qquad (32)$$

Note vehicles j and k are not necessarily neighbors. However, since $z_j(t) - z_k(t) \equiv z_j(0) - z_k(0) - [z_k(t) - z_k(0)] - [z_j(0) - z_j(t)]$, the distance between vehicles j and k satisfies

$$\begin{aligned}
\|z_j(t) - z_k(t)\| &\geq \|z_j(0) - z_k(0)\| - \|z_k(t) - z_k(0)\| \\
&\quad - \|z_j(t) - z_j(0)\| \\
&\geq \|z_j(0) - z_k(0)\| - \sum_{i=1}^{n} \|z_i(t) - z_i(0)\| \\
&\geq \|z_j(0) - z_k(0)\| - \eta \|\varepsilon(0)\|_{a+1}^a \\
&\quad (\text{By (31)}) \\
&> 0, \quad \forall t \in [0, T_c). \qquad (33)
\end{aligned}$$

The last inequality is by the condition (28). Inequality (33) indicates that the distance between any two vehicles is bounded below by a positive constant for all $t \in [0, T_c)$. Clearly (32) conflicts with (33). Thus we have $T_c = +\infty$ and collision avoidance between any vehicles can be ensured. □

Remark 6. As shown in (32) and (33), it is not assumed that vehicles j and k are neighbors. Hence collision avoidance is guaranteed between any vehicles no matter if they are neighbors or not.

We next summarize Propositions 1–3 and give the main stability results as below.

Theorem 1. *Under Assumptions 1 and 2, the equilibrium $\varepsilon = 0$ is locally exponentially stable by control law (4) if $a = 1$, and locally finite-time stable if $a \in (0, 1)$. Collision avoidance between any vehicles (no matter if they are neighbors or not) is locally guaranteed.*

Proof. By Propositions 2 and 3, we have

$$\dot{V} \leq -\frac{K}{\gamma} V^{\frac{2a}{1+a}}, \quad \forall t \in [0, +\infty), \qquad (34)$$

given sufficiently small $\varepsilon(0)$. From (34) we conclude: (i) If $a \in (0, 1)$ and hence $2a/(1+a) \in (0, 1)$, the solution to (4) starting from $\Omega(V(\varepsilon_0))$ converges to $\varepsilon = 0$ in finite time [31, Theorem 4.2]. (ii) If $a = 1$ and hence $2a/(1+a) = 1$, the equilibrium $\varepsilon = 0$ is locally exponentially stable [32, Theorem 3.1]. Collision avoidance has already been proved in Proposition 3. □

Remark 7. As shown in Propositions 1–3, if ε_0 satisfies (20), (28) and $V(\varepsilon_0) \leq 1$, then the convergence and collision avoidance can be guaranteed. Note the right hand side of (20) is less than one. Hence (20) implies $V(\varepsilon_0) \leq 1$. As a result, we can obtain a convergence region from (20) and (28). But this convergence region may be conservative. The real convergence region is not necessarily small, which will be illustrated by simulations.

Up to this point, we have been primarily focusing on the convergence of $\varepsilon(t)$. It should be noted that the convergence of $\varepsilon(t)$ does not simply imply the formation $\{z_i(t)\}_{i=1}^n$ converges to a finite final position. But this issue can be solved by the exponential or finite-time convergence rate. Specifically, control law (4) implies that $z_i(t) = z_i(0) + \int_0^t \sigma_i(g_i - g_{i-1})$. Since ε_i converges to zero exponentially or in finite time, the function $\sigma_i(g_i - g_{i-1})$ is integrable even if $t \to +\infty$. As a result, $\{z_i(t)\}_{i=1}^n$ will converge to a finite position and control law (4) successfully solves Problem 1.

Remark 8. The exponential or finite-time stability not only shows the fast convergence rate of the proposed control law, but also is necessarily useful for proving the finite position of the final converged formation. It is notable that similar problems also appear in control of distance-constrained formations [36, Section V], where the exponential convergence rate of distance dynamics is first proved and then used to prove the formation converging to a finite final position.

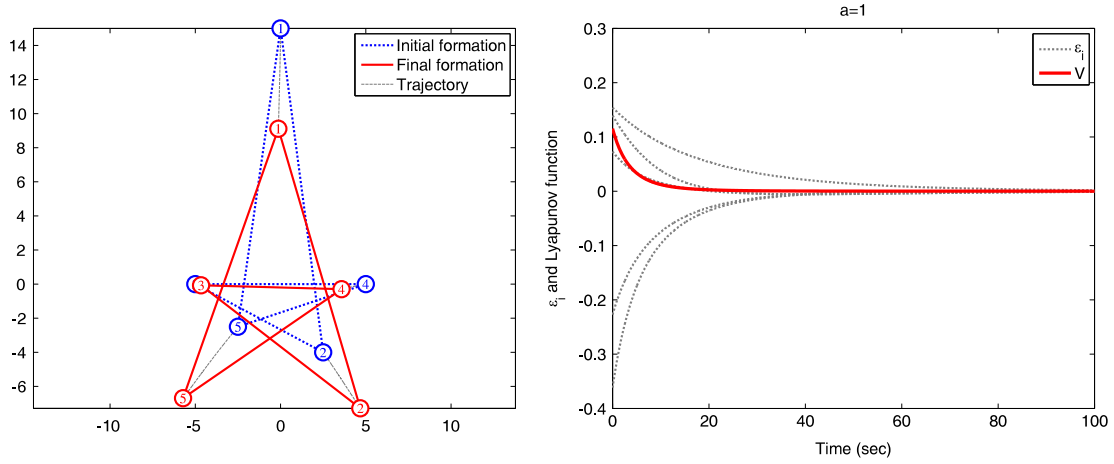

(a) $a = 1$.

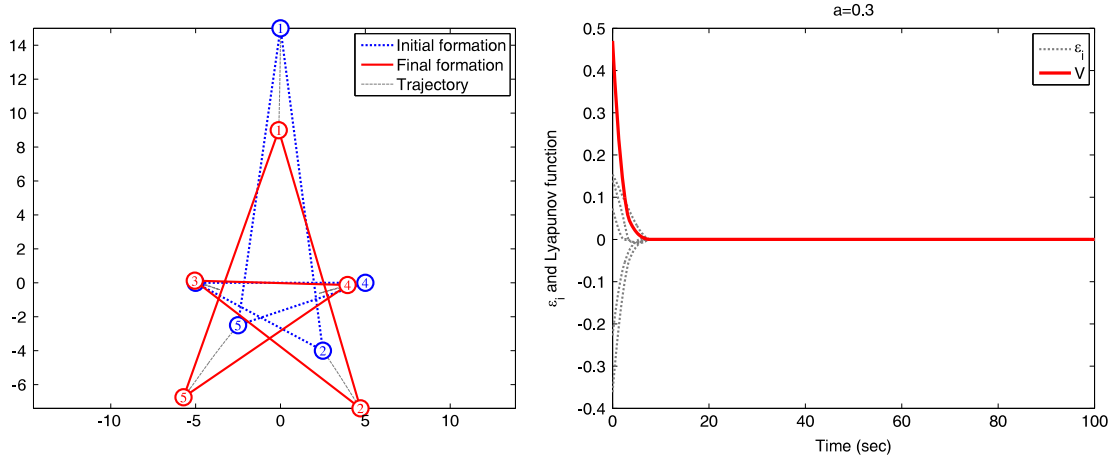

(b) $a = 0.3$.

Fig. 3. Formation and angle error evolution with $n = 5$ and $\theta_1^* = \cdots = \theta_n^* = 36^\circ$.

At last, we characterize a number of important behaviors of the formation evolution. (i) Inequality (27) intuitively indicates that the final converged formation would not move far away from the initial formation if the initial angle errors are small. (ii) From control law (4), it is obvious that $\dot{z} = 0$ if $\varepsilon = 0$. It intuitively means that the vehicles will stop moving once the angles achieve the desired values. (iii) Another important behavior of the formation is that $\dot{z} = 0$ if $\dot{\varepsilon} = 0$. That is because $\dot{\varepsilon} = 0 \Rightarrow \dot{V} = 0 \Rightarrow V = 0 \Rightarrow \varepsilon = 0 \Rightarrow \dot{z} = 0$. The intuitive interpretation is that control law (4) cannot change the positions of the vehicles without changing the angles in the formation.

6. Simulations

Simulations are presented in this section to verify the effectiveness and robustness of the proposed control law.

The desired formation in Fig. 3 is a non-convex star polygon with $n = 5$. The angle at each vertex in the desired formation is $\theta_1^* = \cdots = \theta_5^* = 36^\circ$. As can be seen, the proposed control law can effectively reduce the angle errors. The desired formation in Fig. 4 is a ten-side polygon, where the angle at each vertex is $\theta_1^* = \cdots = \theta_{10}^* = 144^\circ$. In the stability analysis, we assume the initial error $\varepsilon(0)$ is sufficiently small such that $\theta_i, \theta_i^* \in (0, \pi)$ or $(\pi, 2\pi)$ for all points in $\Omega(V(\varepsilon_0))$. However, this assumption is not satisfied in the example where $\theta_i(0) = \pi$ for $i = 2, 3, 7, 8, 10$ and $\theta_5(0) \in (\pi, 2\pi)$ but $\theta_5^* \in (0, \pi)$. As can be seen, the desired formation can still be achieved. The simulation suggests the convergence region of the desired formation by the proposed control law is not necessarily small. As shown in both Figs. 3 and 4, the angle errors and the Lyapunov function converge to zero in finite time if $a < 1$.

Fig. 5 demonstrates the robustness of the proposed control law against measurement noises and vehicle motion failure. In Fig. 5(b), we add an error to each ε_i to simulate measurement noises. Each error is randomly drawn from a normal distribution with mean 0 and standard deviation 1. In Fig. 5(b), vehicle 4 fails to move. As can be seen, the proposed control law still performs well in the presence of measurement noises or motion failure of one vehicle.

7. Conclusions

This paper studied a relatively new formation control topic: distributed control of formations with angle constraints using bearing-only measurements. We proved that the proposed control law can locally stabilize cyclic formations exponentially or in finite time. Collision avoidance between any vehicles can also be locally guaranteed. The stability analysis based on Lyapunov approaches should be useful for future research on more complicated bearing-based formation control problems.

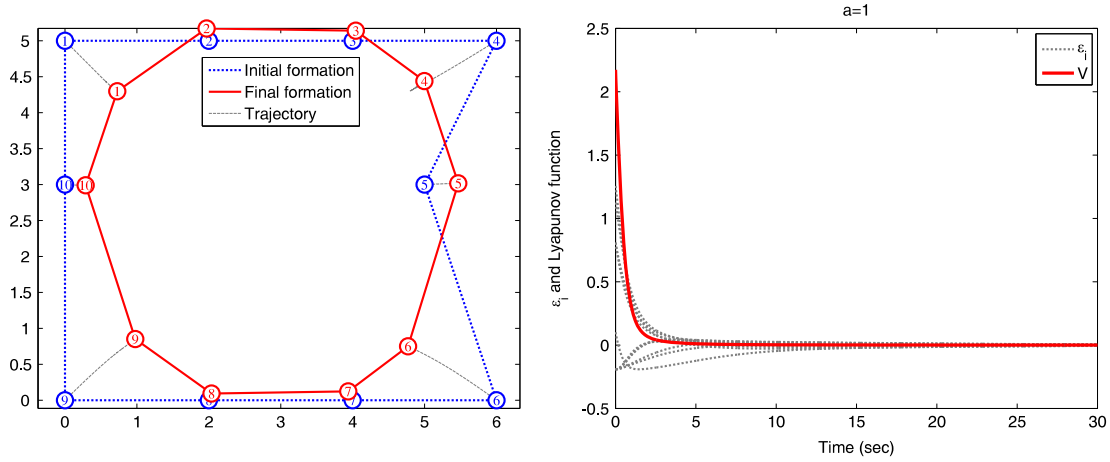

(a) $a = 1$.

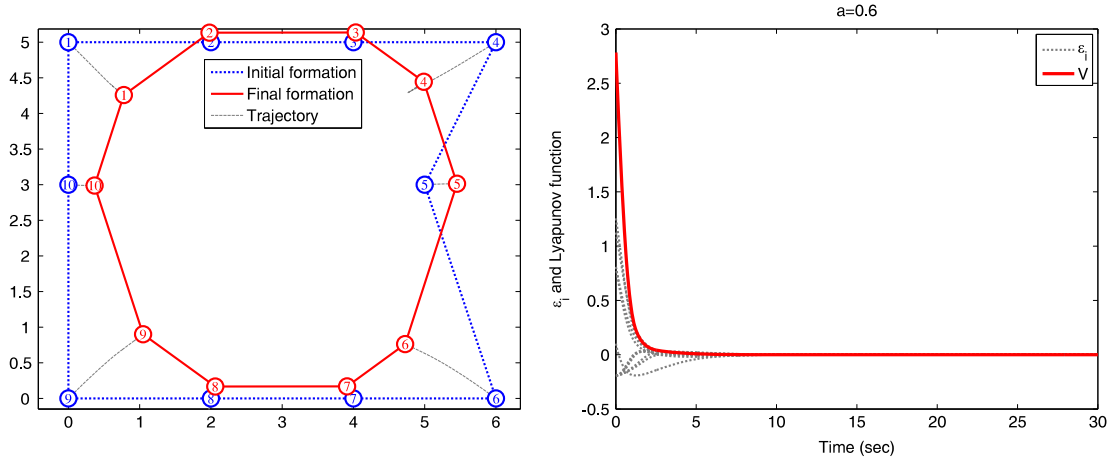

(b) $a = 0.6$.

Fig. 4. Formation and angle error evolution with $n = 10$ and $\theta_1^* = \cdots = \theta_n^* = 144°$.

The work in this paper is a first step towards solving generic bearing-based formation control problems. There are several important directions for future research. Firstly, this paper only considered cyclic formations; formations with more complicated underlying graphs need to be studied in the future. Secondly, in order to control the formation scale, bearing-only constraints and measurements would be insufficient; distance constraints and measurements need be introduced. Distributed control of formations with mixed bearing and distance constraints using mixed measurements is of both theoretical and practical importance.

Appendix A. Proof of Lemma 1

By orthogonally projecting $x \in \mathcal{U}$ to $\mathbf{1}$ and the orthogonal complement of $\mathbf{1}$, we decompose x as

$$x = x_0 + x_1,$$

where $x_0 \in \text{Null}(A)$ and $x_1 \perp \text{Null}(A)$. Let φ be the angle between $\mathbf{1}$ and x. Then we have $\|x_0\| = \cos\varphi\|x\|$ and $\|x_1\| = \sin\varphi\|x\|$. As a result,

$$\begin{aligned} x^{\mathrm{T}}Ax &= x_1^{\mathrm{T}}Ax_1 \\ &\geq \lambda_2(A)x_1^{\mathrm{T}}x_1 \\ &= \lambda_2(A)\sin^2\varphi\|x\|^2. \end{aligned} \tag{35}$$

By the definition of $\mathcal{U}$, any x in $\mathcal{U}$ would not be in span$\{\mathbf{1}\}$. That means $\varphi \neq 0$ or π and hence $\sin\varphi \neq 0$. We next identify the positive infimum of $\sin\varphi$.

Define $\bar{\mathcal{U}}_p = \{x \in \mathbb{R}^n : x \neq 0$ and nonzero entries of x are all positive$\}$ and $\bar{\mathcal{U}}_n = \{x \in \mathbb{R}^n : x \neq 0$ and nonzero entries of x are all negative$\}$. Let $\bar{\mathcal{U}} = \{0\} \cup \bar{\mathcal{U}}_p \cup \bar{\mathcal{U}}_n$. Clearly $\mathcal{U} \cup \bar{\mathcal{U}} = \mathbb{R}^n$. It is easy to see $\bar{\mathcal{U}}$ is a closed set and hence $\mathcal{U}$ is an open set. Fig. 6 shows a 2D example to illustrate the above notations. Denote $\partial\mathcal{U}$ as the boundary of $\mathcal{U}$. The vector $\mathbf{1} \in \bar{\mathcal{U}}$ is isolated from any $x \in \mathcal{U}$ by $\partial\mathcal{U}$. Then we have $\inf_{x\in\mathcal{U}}\varphi = \min_{x\in\partial\mathcal{U}}\angle(x, \mathbf{1})$ and $\sup_{x\in\mathcal{U}}\varphi = \max_{x\in\partial\mathcal{U}}\angle(x, \mathbf{1})$. In fact, the boundary $\partial\mathcal{U}$ is formed by the hyper-planes $[x]_i = 0$ with $i \in \{1, \ldots, n\}$. Denote $p_i \in \mathbb{R}^n$ as the orthogonal projection of $\mathbf{1}$ on the hyper-plane $[x]_i = 0$. Then $\min_{x\in\partial\mathcal{U}}\angle(x, \mathbf{1}) = \angle(p_i, \mathbf{1})$ and $\max_{x\in\partial\mathcal{U}}\angle(x, \mathbf{1}) = \angle(-p_i, \mathbf{1})$. Note the ith entry of p_i is zero and the others are one. It can be calculated that $\cos\angle(\pm p_i, \mathbf{1}) = \pm\sqrt{n-1}/\sqrt{n}$ and hence $\sin\angle(\pm p_i, \mathbf{1}) = 1/\sqrt{n}$. Thus

$$\inf_{x\in\mathcal{U}}\sin\varphi = \frac{1}{\sqrt{n}},$$

substituting which into (35) yields

$$\inf_{x\in\mathcal{U}}\frac{x^{\mathrm{T}}Ax}{x^{\mathrm{T}}x} = \frac{\lambda_2(A)}{n}. \quad \square$$

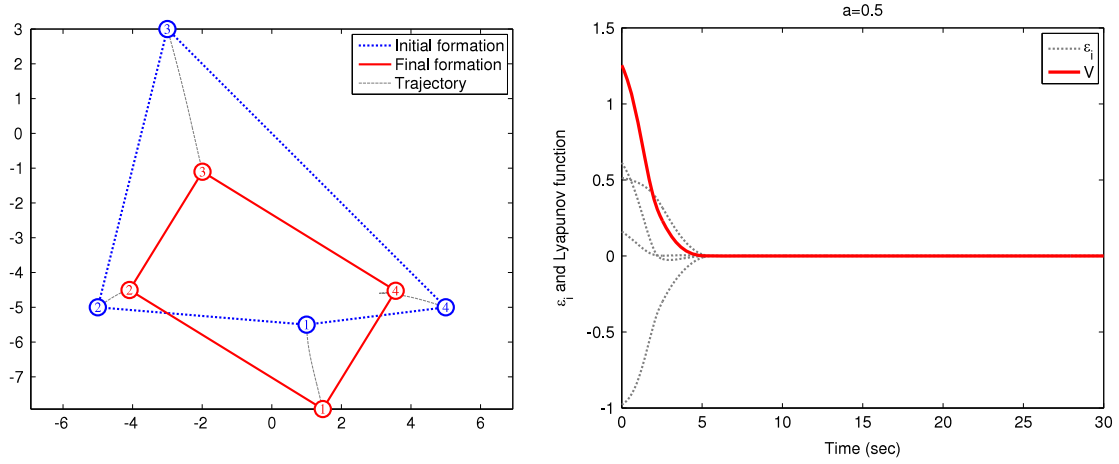

(a) Ideal case.

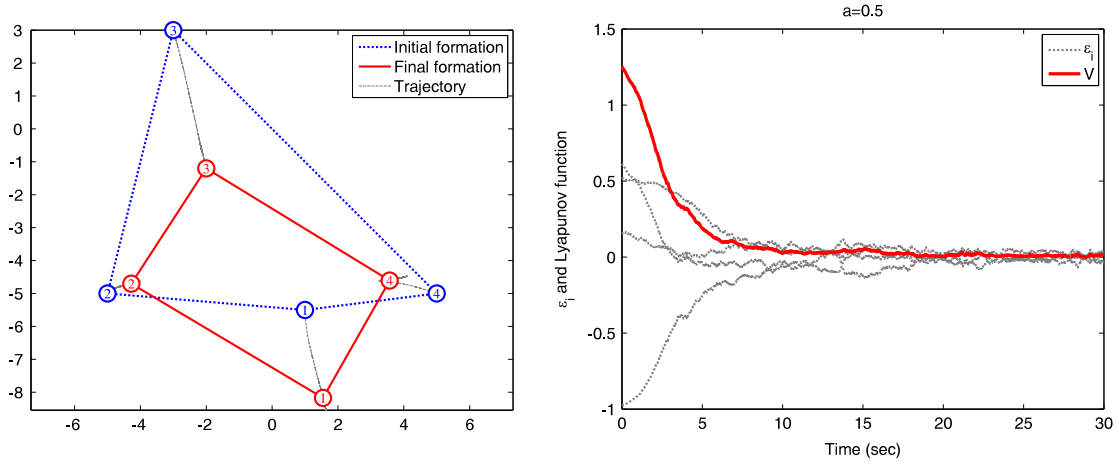

(b) In the presence of measurement noise.

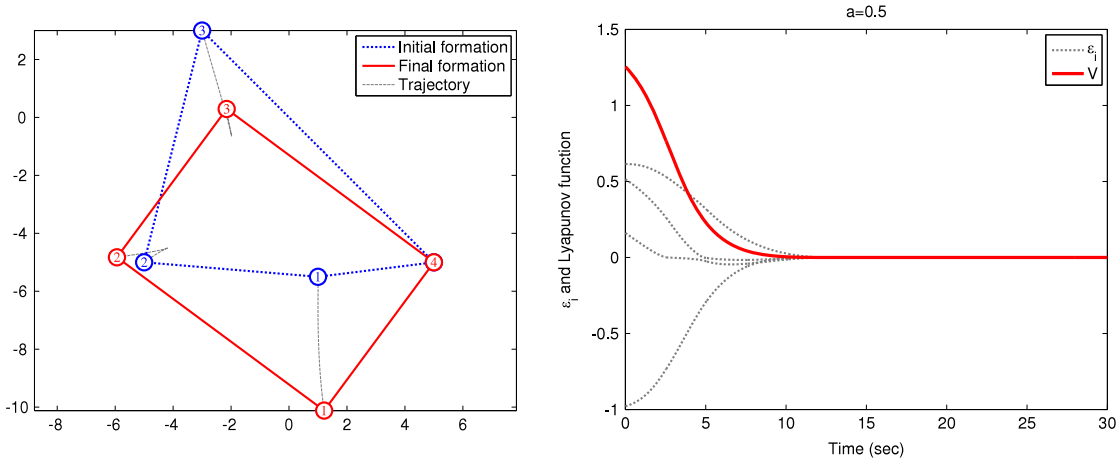

(c) In the presence of vehicle motion failure (Vehicle 4 fails to move).

Fig. 5. An illustration of the robustness of the proposed control law against measurement noise and vehicle motion failure. $n = 4$ and $\theta_1^* = \cdots = \theta_4^* = 90°$.

Appendix B. Proof of Lemma 2

The proof consists of three steps.

Step 1: Prove the special case of $\alpha = 1$ and $k \in (0, 1)$.

The idea of the proof is to repeatedly utilize inequality (1) and the following inequality

$$x(t) \le x(0) + \int_0^t |\dot{x}(\tau)| \mathrm{d}\tau. \tag{36}$$

First of all, because $x > 0$, we have $-k/x < 0$ and hence by (1) we have

$$|\dot{x}(t)| \le \exp(0) = 1,$$

substituting which into (36) gives

$$x(t) \le x(0) + \int_0^t 1 \mathrm{d}\tau = t + c,$$

where $c = x(0)$. Substituting the above inequality back into (1) yields

$$\begin{aligned} |\dot{x}(t)| &\le \exp\left(\int_0^t -\frac{k}{\tau + c}\mathrm{d}\tau\right) \\ &= \exp\left(-k \ln \frac{t+c}{c}\right) \\ &= \left(\frac{c}{t+c}\right)^k. \end{aligned}$$

Again by (36) we have

$$\begin{aligned} x(t) &\le x(0) + \int_0^t \left(\frac{c}{\tau + c}\right)^k \mathrm{d}\tau \\ &= x(0) + \frac{c^k}{1-k}\left[(t+c)^{1-k} - c^{1-k}\right] \\ &< \frac{c^k}{1-k}(t+c)^{1-k}, \end{aligned} \tag{37}$$

where the last inequality uses the fact $c = x(0)$, $1 - k < 1$ and hence $x(0) - c/(1-k) < 0$. Denote $\mu = (1-k)/c^k$. Substituting (37) into (1) gives

$$\begin{aligned} |\dot{x}(t)| &< \exp\left(\int_0^t -\mu k(\tau + c)^{k-1}\mathrm{d}\tau\right) \\ &= \exp\left(-\mu(t+c)^k + \mu c^k\right) \\ &= e^{1-k}e^{-\mu(t+c)^k}. \end{aligned}$$

One more by (36) we have

$$\begin{aligned} x(t) &\le x(0) + e^{1-k}\int_0^t e^{-\mu(\tau+c)^k}\mathrm{d}\tau \\ &\le x(0) + e^{1-k}\int_0^{+\infty} e^{-\mu(\tau+c)^k}\mathrm{d}\tau. \end{aligned} \tag{38}$$

Let $s = \mu(\tau + c)^k$. Then $\mathrm{d}\tau = (1/k)\mu^{-1/k}s^{1/k-1}\mathrm{d}s$. The above integral becomes

$$\begin{aligned} \int_0^{+\infty} e^{-\mu(\tau+c)^k}\mathrm{d}\tau &= \frac{1}{k}\mu^{-\frac{1}{k}}\int_{\mu c^k}^{+\infty} e^{-s}s^{\frac{1}{k}-1}\mathrm{d}s \\ &< \frac{1}{k}\mu^{-\frac{1}{k}}\int_0^{+\infty} e^{-s}s^{\frac{1}{k}-1}\mathrm{d}s \\ &= \frac{1}{k}\mu^{-\frac{1}{k}}\Gamma\left(\frac{1}{k}\right), \end{aligned} \tag{39}$$

where $\Gamma(1/k)$ is the well-known *Gamma function* and it has a positive value at $1/k > 0$. By substituting (39) into (38), we find a finite upper bound for $x(t)$ as

$$x(t) < \gamma = x(0) + \frac{1}{k}\mu^{-\frac{1}{k}}e^{1-k}\Gamma\left(\frac{1}{k}\right).$$

Step 2: Prove the special case of $\alpha = 1$ and $k \in [1, +\infty)$.

Consider a constant $k_0 \in (0, 1)$. Then $k > k_0$. Since $x(t) > 0$ for all $t \in [0, +\infty)$, we have

$$\int_0^t -\frac{k}{x(\tau)}\mathrm{d}\tau < \int_0^t -\frac{k_0}{x(\tau)}\mathrm{d}\tau,$$

which implies

$$|\dot{x}(t)| \le \exp\left(\int_0^t -\frac{k}{x(\tau)}\mathrm{d}\tau\right) < \exp\left(\int_0^t -\frac{k_0}{x(\tau)}\mathrm{d}\tau\right).$$

Then by Step 1 there exists a finite upper bound γ such that $x(t) < \gamma$ for all $t \in [0, +\infty)$.

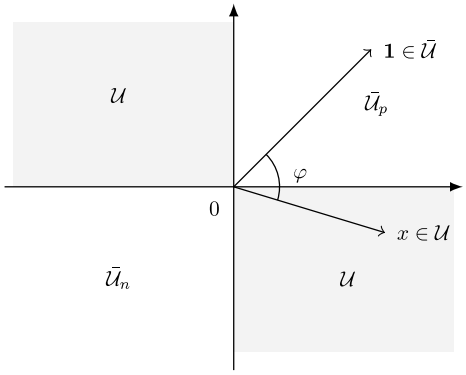

Fig. 6. A 2D illustration for the proof of Lemma 1.

Step 3: Prove the generic case of $\alpha \in (0, +\infty)$ and $k \in (0, +\infty)$.

Note the combination of Step 1 and Step 2 indicates that $x(t)$ is bounded above if $\alpha = 1$ and $k \in (0, +\infty)$. When $\alpha \in (0, +\infty)$, inequality (1) can be rewritten as

$$\left|\left(\frac{x(t)}{\alpha}\right)'\right| \le \exp\left(\int_0^t -\frac{k/\alpha}{x(\tau)/\alpha}\mathrm{d}\tau\right).$$

By Step 1 and Step 2, we know $x(t)/\alpha$ is bounded above, and so is $x(t)$. □

Appendix C. Proof of Lemma 5

(i) Denote $G_i = [g_i, g_i^\perp] \in \mathbb{R}^{2\times 2}$. It is easy to examine that G_i is an orthogonal matrix satisfying $G_i^{\mathrm{T}}G_i = G_iG_i^{\mathrm{T}} = I$. Hence we have

$$g_ig_i^{\mathrm{T}} + g_i^\perp(g_i^\perp)^{\mathrm{T}} = G_iG_i^{\mathrm{T}} = I.$$

Thus $g_i^\perp(g_i^\perp)^{\mathrm{T}} = I - g_ig_i^{\mathrm{T}} = P_i$.

(ii) $(g_i^\perp)^{\mathrm{T}}g_j = g_i^{\mathrm{T}}R^{\mathrm{T}}(\pi/2)g_j = g_i^{\mathrm{T}}R(-\pi/2)g_j = g_i^{\mathrm{T}}R(-\pi)R(\pi/2)g_j$
$= g_i^{\mathrm{T}}R(-\pi)g_j^\perp = g_i^{\mathrm{T}}(-I)g_j^\perp = -(g_j^\perp)^{\mathrm{T}}g_i$.

(iii) By the definition of θ_i, we have $g_i = R(\theta_i)(-g_{i-1})$ and hence $g_{i-1} = -R(-\theta_i)g_i$. Then

$$\begin{aligned} (g_i^\perp)^{\mathrm{T}}g_{i-1} &= -g_i^{\mathrm{T}}R\left(-\frac{\pi}{2}\right)R(-\theta_i)g_i \\ &= -g_i^{\mathrm{T}}R\left(-\frac{\pi}{2} - \theta_i\right)g_i \\ &= -\|g_i\|\left\|R\left(-\frac{\pi}{2} - \theta_i\right)g_i\right\|\cos\left(-\frac{\pi}{2} - \theta_i\right) \\ &= \sin\theta_i. \end{aligned}$$

Then it is straightforward to have the rest results in Lemma 5(iii). □

References

[1] A.K. Das, R. Fierro, V. Kumar, J.P. Ostrowski, J. Spletzer, C.J. Taylor, A vision-based formation control framework, IEEE Transactions on Robotics and Automation 18 (5) (2002) 813–825.

[2] N. Moshtagh, N. Michael, A. Jadbabaie, K. Daniilidis, Vision-based, distributed control laws for motion coordination of nonholonomic robots, IEEE Transactions on Robotics 25 (4) (2009) 851–860.

[3] G.L. Mariottini, F. Morbidi, D. Prattichizzo, N.V. Valk, N. Michael, G. Pappas, K. Daniilidis, Vision-based localization for leader–follower formation control, IEEE Transactions on Robotics 25 (6) (2009) 1431–1438.

[4] P. Vela, A. Betser, J. Malcolm, A. Tannenbaum, Vision-based range regulation of a leader–follower formation, IEEE Transactions on Control Systems Technology 17 (2) (2009) 442–448.

[5] F. Lin, X. Dong, B.M. Chen, K.Y. Lum, T.H. Lee, A robust real-time embedded vision system on an unmanned rotorcraft for ground target following, IEEE Transactions on Industrial Electronics 59 (2) (2012) 1038–1049.

[6] Y. Ma, S. Soatto, J. Kosecka, S. Sastry, An Invitation to 3D Vision, Springer, New York, 2004.

[7] N. Moshtagh, N. Michael, A. Jadbabaie, K. Daniilidis, Bearing-only control laws for balanced circular formations of ground robots, in: Proceedings of Robotics: Science and Systems, Zurich, Switzerland, 2008.

[8] M. Basiri, A.N. Bishop, P. Jensfelt, Distributed control of triangular formations with angle-only constraints, Systems & Control Letters 59 (2010) 147–154.
[9] A.N. Bishop, A very relaxed control law for bearing-only triangular formation control, in: Proceedings of the 18th IFAC World Congress, Milano, Italy, 2011, pp. 5991–5998.
[10] A.N. Bishop, Distributed bearing-only quadrilateral formation control, in: Proceedings of the 18th IFAC World Congress, Milano, Italy, 2011, pp. 4507–4512.
[11] T. Eren, Formation shape control based on bearing rigidity, International Journal of Control 85 (9) (2012) 1361–1379.
[12] A. Franchi, P.R. Giordano, Decentralized control of parallel rigid formations with direction constraints and bearing measurements, in: Proceedings of the 51st IEEE Conference on Decision and Control, Hawaii, USA, 2012, pp. 5310–5317.
[13] M. Cao, C. Yu, B.D.O. Anderson, Formation control using range-only measurements, Automatica 47 (2011) 776–781.
[14] M. Cao, A.S. Morse, An adaptive approach to the range-only station-keeping problem, International Journal of Adaptive Control and Signal Processing 26 (2012) 757–777.
[15] R. Olfati-Saber, R.M. Murray, Distributed cooperative control of multiple vehicle formations using structural potential functions, in: Proceedings of the 15th IFAC World Congress, Barcelona, Spain, 2002.
[16] L. Krick, M.E. Broucke, B.A. Francis, Stabilization of infinitesimally rigid formations of multi-robot networks, International Journal of Control 82 (3) (2009) 423–439.
[17] F. Dörfler, B. Francis, Geometric analysis of the formation problem for autonomous robots, IEEE Transactions on Automatic Control 55 (10) (2010) 2379–2384.
[18] C. Yu, B.D.O. Anderson, S. Dasgupta, B. Fidan, Control of minimally persistent formations in the plane, SIAM Journal on Control and Optimization 48 (1) (2009) 206–233.
[19] T.H. Summers, C. Yu, S. Dasgupta, B.D.O. Anderson, Control of minimally persistent leader-remote-follower and coleader formations in the plane, IEEE Transactions on Automatic Control 56 (12) (2011) 2778–2792.
[20] H. Huang, C. Yu, Q. Wu, Autonomous scale control of multiagent formations with only shape constraints, International Journal of Robust and Nonlinear Control 23 (7) (2013) 765–791.
[21] A.N. Bishop, Stabilization of rigid formations with direction-only constraints, in: Proceedings of the 50th IEEE Conference on Decision and Control and European Control Conference, Orlando, FL, USA, 2011, pp. 746–752.
[22] T. Eren, W. Whiteley, A.S. Morse, P.N. Belhumeur, B.D.O. Anderson, Sensor and network topologies of formations with direction, bearing and angle information between agents, in: Proceedings of the 42nd IEEE Conference on Decision and Control, Hawaii, USA, 2003, pp. 3064–3069.
[23] A.N. Bishop, T.H. Summers, B.D.O. Anderson, Stabilization of stiff formations with a mix of direction and distance constraints, in: Proceedings of the 2013 IEEE Multi-Conference on Systems and Control, 2013, in press.
[24] S.C. Nardone, A.G. Lindgren, K.F. Gong, Fundamental properties and performance of conventional bearings-only target motion analysis, IEEE Transactions on Automatic Control 29 (9) (1984) 775–787.
[25] J. Cortés, Global and robust formation-shape stabilization of relative sensing networks, Automatica 45 (2009) 2754–2762.
[26] C. Godsil, G. Royle, Algebraic Graph Theory, Springer, New York, 2001.
[27] L. Wang, F. Xiao, Finite-time consensus problems for networks of dynamic agents, arXiv:math/0701724.
[28] R.A. Horn, C.R. Johnson, Matrix Analysis, Cambridge University Press, 1985.
[29] J. Cortés, Finite-time convergent gradient flows with applications to network consensus, Automatica 42 (2006) 1993–2000.
[30] J. Cortés, Discontinuous dynamical systems, IEEE Control Systems Magazine 28 (3) (2008) 36–73.
[31] S.P. Bhat, D.S. Bernstein, Finite-time stability of continuos autonomous systems, SIAM Journal on Control and Optimization 38 (3) (2000) 751–766.
[32] W.M. Haddad, V. Chellaboina, Nonlinear Dynamical Systems and Control: A Lyapunov-Based Approach, Princeton University Press, 2008.
[33] F. Xiao, L. Wang, J. Chen, Y. Gao, Finite-time formation control for multi-agent systems, Automatica 45 (2009) 2605–2611.
[34] Y. Cao, W. Ren, Z. Meng, Decentralized finite-time sliding mode estimators and their applications in decentralized finite-time formation tracking, Systems & Control Letters 59 (2010) 522–529.
[35] H.K. Khalil, Nonlinear Systems, third ed., Prentice Hall, 2002.
[36] F. Dörfler, B. Francis, Formation control of autonomous robots based on cooperative behavior, in: Proceedings of the 2009 European Control Conference, Budapest, Hungary, 2009, pp. 2432–2437.